https://ntrs.nasa.gov/search.jsp?R=20140011534 2019-08-31T19:06:21+00:00Z

Remote Recession Sensing of Ablative Heat Shield Materials

Michael W. Winter [i]
University of Kentucky, Department of Mechanical Engineering, Lexington, KY 40506-0503, USA

Margaret Stackpoole [ii]
NASA Ames Research Center, Moffett Field, CA 94035

Anuscheh Nawaz[iii]
Sierra Lobo, Inc., NASA Ames Research Center, Moffett Field, CA, 94035

Gregory Lewis Gonzales [iv]
ERC, Inc., NASA Ames Research Center, Moffett Field, CA, 94035

Thanh Ho[v]
Universities Space Research Association (USRA), NASA Ames Research Center, Moffett Field, CA, 94035

Extended Abstract

Material recession and charring are two major processes determining the performance of ablative heat shield materials. Even in ground testing, the characterization of these two mechanisms relies on measurements of material thickness before and after testing, thus providing only information integrated over the test time. For recession measurements, optical methods such as imaging the sample surface during testing are under investigation[1] but require high alignment and instrument effort, therefore being not established as a standard measurement method. For char depth measurements, the most common method so far consists in investigation of sectioned samples after testing or in the case of Stardust where core extractions were performed to determine char information.[2] In flight, no reliable recession measurements are available, except total recession after recovering the heat shield on ground. Developments of mechanical recession sensors have been started[5] but require substantial on board instrumentation adding mass and complexity. In this work, preliminary experiments to evaluate the feasibility of remote sensing of material recession and possibly char depth through optically observing the emission signatures of seeding materials in the post shock plasma is investigated. It is shown that this method can provide time resolved recession measurements without the necessity of accurate alignment procedures of the optical set-up and without any instrumentation on board of a spacecraft. Furthermore, recession data can be obtained without recovering flight hardware which would be a huge benefit for inexpensive heat shield material testing on board of small re-entry probes, e.g. on new micro-satellite re-entry probes as a possible future application of Cubesats[3] or RBR.[4]

In the spectrally resolved data gathered during the airborne observation campaign of the Stardust sample return capsule, the emission of tracer elements such as sodium, potassium, magnesium, and calcium was observed.[6] Calcium has been found to be present in the preform of the Phenolic Impregnated Carbon Ablator (PICA) forebody TPS material used on Stardust. Magnesium has been assigned to the protective paint of the heat shield. The strong appearance in the observed spectra was surprising, though, since these elements were not major constituents of the PICA material and are only present in trace concentrations. These results have been confirmed in preliminary ground testing of PICA in the NASA Ames arc-jet facilities.[7] Apparently, these tracer elements are able to diffuse against the incoming flow into the boundary layer and eventually into the post-shock layer where they emit substantial radiation due to the high plasma temperatures in this region. The concept of remote ablation sensing uses this effect by seeding the heat shield material at known depths with selected tracer materials. Once recession reaches the seeding depth, the characteristic emission of the seeding elements is expected to

[i] Assistant Professor, University of Kentucky, Department of Mechanical Engineering, 261 Ralph G. Anderson Building, Lexington, KY 40506-0503, USA, Michael.Winter@uky.edu , Associate Fellow AIAA
[ii] Senior Research Scientist, Thermal Protection Materials and Systems Branch, NASA Ames Research Center,
[iii] Senior Aerospace Engineer, Thermo-Physics Facilities Branch, Mail Stop 229-4, Member AIAA.
[iv] Research Engineer, Thermal Protection Materials and Systems Branch, NASA Ames Research Center,.
[v] Research Assistant, Thermo-Physics Facilities Branch, NASA Ames Research Center.

show up in the emission spectra emitted by the post-shock plasma. When the recession exceeds the maximum seeding depth, this emission signature should fade in the observed spectra. Since these signatures are distinguishes from the plasma emission in the spectral domain and due to the diffusion of the seeding material into the boundary and post-shock layer, no particular spatial resolution of the optical system is required as long as the majority of the post-shock system is covered by the collecting optics. A spatial resolution is obtained by restricting the seeding material to a selected position on the sample or heat shield. If the emission spectra are recorded continuously with time, a temporal assignment of a particular recession depth (pre-selected through seeding a defined in-depth position) is possible. To demonstrate this concept, tests with different seeding materials and configurations were done in the Miniature Arc Jet (mARC) facility at NASA Ames.[8]

The mARC Facility

The mARC is a subscale segmented arc heater in which a continuous electrical discharge between electrodes in the arc chamber heats and expands air at a mass flow rate of approximately 0.45 g/s (in this study) to high temperatures and supersonic velocities. The DC arc jet is composed of a cylindrically symmetric geometry consisting of a coolant-cooled thoriated tungsten tipped cathode, a water-cooled copper anode, a constrictor channel, and a converging-diverging nozzle. A schematic of the cross section of the mARC can be seen in Figure 1. In operation, a Hypertherm Max 200 30 kW plasma cutting power supply capable of supplying up to 200 A DC establishes a high current regulated arc. The arc is directed from the cathode tip, through a 1.3 cm diameter constricted arc column channel, and attaches to the anode. Air is swirled into the arc column through injection ports located behind the cathode. A swirling ring is used to stabilize the arc, constrain the hot gas discharge column to the axis of the vortex, and bring the gas into longer and more effective contact with the arc. The resultant constricted arc heats and largely ionizes the air on the centerline of the constrictor and continues to heat the boundary air through radiation and conduction, resulting in a large radial temperature gradient. It is this large radial temperature gradient which allows the centerline temperature of the heated air to be very high without melting the nozzle. After being directed through the arc column, the hot air is then accelerated out through the convergent-divergent nozzle (1 cm exit diameter) forming a plasma column approximately 1.3 cm in diameter.

The mARC uses a cylindrical vacuum chamber of approximately 0.61 m in length and 0.3 m diameter connected to two Leybold Trivac (model # D30A) rotary vane dual stage mechanical vacuum pumps capable of providing base pressures in the 0.001 kPa (10 mTorr) range. Chamber background pressures consistently reached approximately 2.67 kPa (20 Torr) during operation. The mARC anode was water cooled by a Goulds Pumps e-SV Series vertical multi-stage pump capable of flowing water at 7.885 kg/s. A cooled diffuser was placed at the lower end of the chamber to prevent overheating of the chamber walls due to the high flow temperatures. The layout of the facility can be seen in Figure 2.

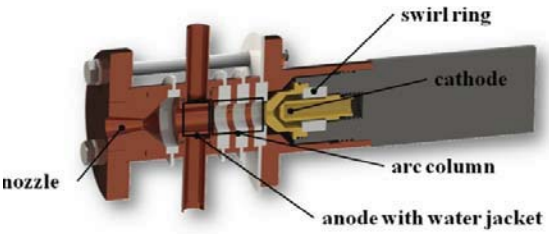

Figure 1: Cross sectional schematic of the mARC[8]

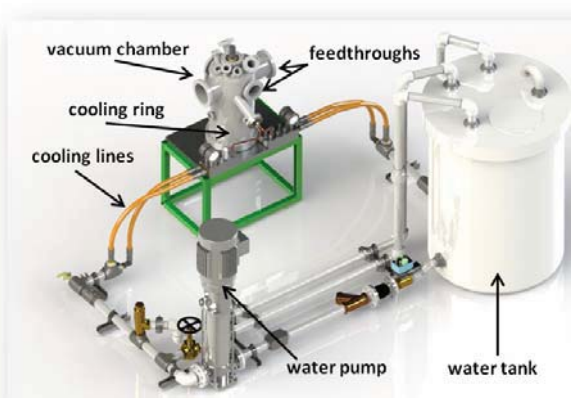

Figure 2: The mARC vacuum facility[8]

Sample Geometry and Seeding Procedure

PICA was chosen as the baseline material to demonstrate the seeding concept as PICA is a heritage TPS material and the baseline forebody heatshield for OSIRIS REx. Additionally, PICA is a low-density material that is easily machined making it suitable for this demonstration experiment, and PICA has limited constituents thereby not adding further to the emission spectra. Two sets of PICA coupons were evaluated; 6.35mm (0.25") diameter cylindrical (Figure 3) and 8.38mm (0.33") rectangular coupons (Figure 4). The smaller coupons were more challenging to align during testing, however the larger coupons were successfully tested.

A series of seeding materials were evaluated including, metals, oxides and salts of Al, Ti, Mg and Si. Sodium chloride was also included. All seeding materials were in powder form having a high surface area (mean powder diameter of a few

microns) The seeding materials were extruded with a polymer matrix to form seeding rods. The PICA coupons were drilled at given locations and the seeding rods were inserted into the PICA and sealed using a PICA like paste allowing the seeding material to be encapsulated within the PICA. An example of the seeded materials inserted in the PICA prior to encapsulating is shown in Fig. 3. Due to limited test time all seeding materials were not evaluated in the mARC facility. The results presented will focus on samples seeded with NaCl and MgCl.

(a) **(b)**

Figure 3: (a) PICA cylindrical test coupons (6.35mm diameter) (b) seeded materials inserted in the PICA prior to encapsulating

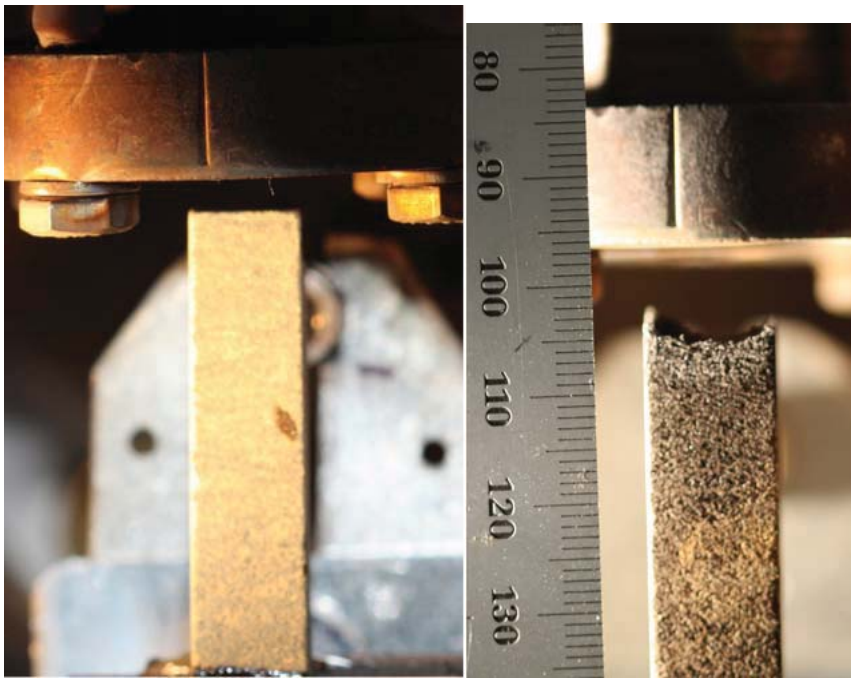

(a) **(b)**

Figure 4: Typical PICA rectangular test coupons (a) per test and (b) post test

Optical Set-up and Results

The emission was taken using a focal point imaging system with a 25 mm (2 inch) spherical mirror with a focal length of 305 mm (12 inch) providing a mostly collimated beam with the mirror diameter. The light was focused on a 200µm optical fiber and detected with an miniaturized spectrometer (Avantes AvaSpec-3648-USB2-UA, nominal wavelength range 180-1100nm). The f number of the fiber (numerical aperture n_A=0.22) was matched using an aperture between mirror and fiber. The beam cross section covered the arc-jet nozzle exit with its upper edge, the virgin sample surface placed approximately at 10mm from the upper edge of the detection beam. The alignment was done using a HeNe laser which was reversely fed into the collimating system.

During recession, the surface did move through the beam center towards the lower edge. In pretests, the set-up sensitivity over the beam cross section was found to change moderately depending on the fiber orientation. Therefore, it cannot to be excluded that the sensitivity to light coming from the receding surface might change with test time, though considered minor due to the experience during the pretests. The measurements were calibrated to absolute intensities using an integrating sphere.

Data acquisition was started shortly before the sample was inserted with acquisition times of 15ms and a data rate of ~67Hz. During analysis, data were averaged to one point every 0.105 seconds. Background noise was measured separately after the test and was subtracted from the measured data. All data were wavelength calibrated through measurements of a Hg calibration lamp, and intensity calibrated to spectral radiance (W cm^{-2} sr^{-1} nm^{-1}) through measurements of a halogen integrating sphere and a Deuterium lamp. Synthetic spectra of Mg and Na were generated based on NIST tabulated spectroscopic data using Boltzmann distributions and a series of temperatures. The data shown for comparison were generated using Boltzmann distributions of the electronically excited levels for a temperature of 9000K which was arbitrarily chosen to show also weaker lines in the spectrum.
The continuum emission of the glowing probe showed an increase with test time which may be caused by a change in visible glowing surface area due to unsymmetrical recession or/and through a non uniform set-up sensitivity over the detection beam cross section. CN emission around 390 nm was detected throughout the whole test with decreasing intensity with test time. Emission lines of Mg (280nm, 285nm, and 518nm) and Na (568nm, 589nm, and 819nm) were identified in the arc-jet plasma. The time trace of the spectral emission is shown in Fig. 5, the identification of the Mg lines is demonstrated in Fig. 6.

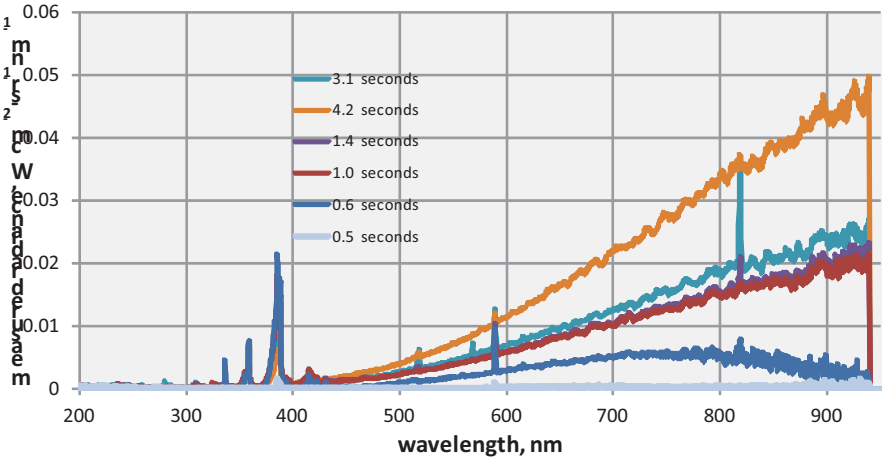

Figure 5: Selected emission spectra for increasing test time.

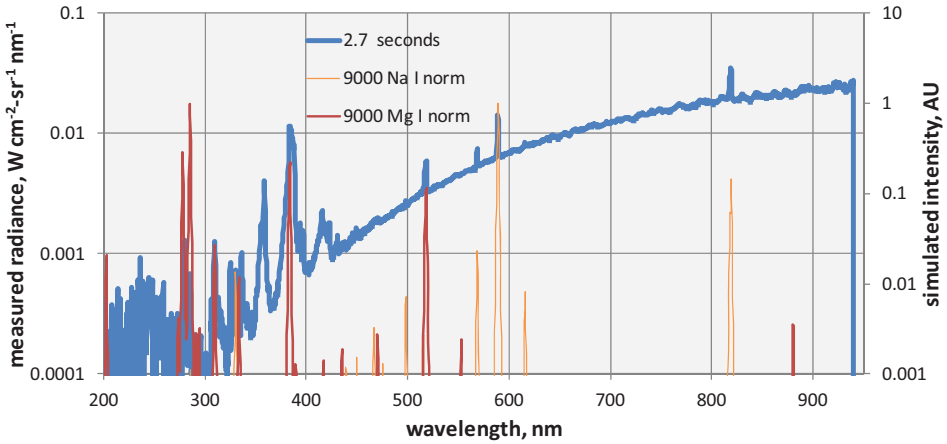

Figure 6: Measured spectra at about 2.3 seconds after sample insertion in comparison to synthetic spectra of sodium and magnesium derived from NIST tabulated spectroscopic constants.

All identified lines started showing up about 1 second after sample insertion and disappeared at roughly 4 seconds after insertion, as illustrated in Fig. 7 by the integrated line emissions. Only the Na line at 589nm was present right after sample insertion, however, it disappeared together with the other emission lines. The fact that only this individual Na line showed up at the beginning of the test and not the ones observed later indicates a significantly lower excitation temperature for the sodium emission at the beginning of the test in comparison to the later emission which seems clearly related to ablation processes (as indicated by the other observed atom lines). It might be that residual sodium from the ambient air is responsible for this emission. Another explanation might be sodium on the sample surface which would explain why the emission shows a local maximum right at the beginning followed by a decreasing trend.

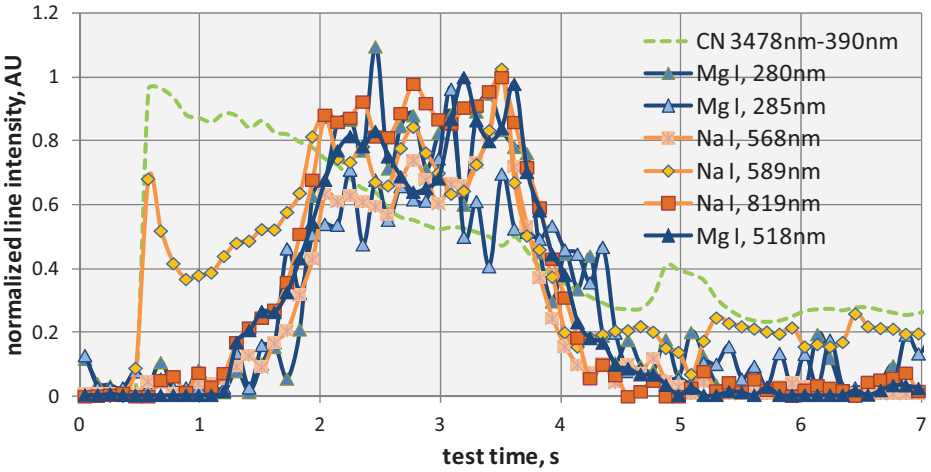

Figure 7: Time trace of spectrally integrated line emission of sodium and magnesium.

Conclusions

The tests in the mARC facility demonstrated the feasibility of a remote ablation sensor during arc-jet testing. The emission signatures of the seeding elements (Mg and Na) were detected about 1.5 seconds after the article was inserted into the plasma flow and faded out after about 3 seconds. The 589 nm emission line of Na was present during the whole test time, though, which may be assigned to residual sodium in the ambient air. Parametric studies will have to be conducted to determine optimum seeding amounts and strategies as well as further suitable seeding materials. For these investigations, small plasma facilities are well suited to avoid high testing costs. Once suitable seeding materials and their emission signatures are sufficiently characterized, testing in qualification facilities capable to produce re-entry relevant conditions and spatially and temporarily constant recession rates are recommended to quantitatively investigate the sensing method and relate the results to traditional recession measurements. One attractive application of this method is the seeding of re-entry capsule heat shields to gather in-flight data using airborne or ground based observation of the re-entry, one desirable candidate mission being the upcoming OSIRIS-Rex mission by NASA Goddard and Lockheed Martin. However, small re-entry probes for inexpensive flight testing of heat shield materials would be a suitable application, too, since remote sensing would enable data acquisition of heat shield performance and recession without the need of recovering the flight hardware.

Acknowledgments

The present work was supported by NASA Contract NNA10DE12C to ERC, Inc. The authors would like to thank Dr. George Raiche (Chief, Thermophysics Facilities Branch, NASA ARC) for generously providing test time in the mARC facility for the experiment, and Dr. Dean Kontinos (Chief, Entry Systems & Technology Division, NASA ARC), Dr. Ethiraj Venkatapathy, Dr. Jim Arnold, and Dr. Jay Grinstead for their support during the design of system and testing, and to the arc-jet operation crew for support during the test campaign.

References

[1] Edward T Schairer and James T Heineck, “Photogrammetric recession measurements of ablative materials in arcjets” 2010 Meas. Sci. Technol. **21** 025304.

[2] Dean A. Kontinos, Mairead Stackpoole, “Post-Flight Analysis of the Stardust Sample Return Capsule Earth Entry,”AIAA 2008-1197, 46th Aerospace Sciences Meeting, Reno, Jan. 2008

[3] Bryan Chan, Nicole Bauer, Jessica R. Juneau, Stephanie Stout, Kento Masuyama, Dave Spencer, “Recovery of in-space Cubesat Experiments (RICE) Project,” Intenational Planetary Probe Workshop 2010 (IPPW-7), 14-18 June, Barcelona, Spain.

[4] Weaver, Michael A., and William H. Ailor. "Reentry Breakup Recorder: Concept, Testing, Moving Forward," AIAA Space 2012 Conference and Exposition, 11 - 13 September 2012, Pasadena, California.

[5] Tomomi Oishi, Edward Martinez, “Development and Application of a TPS Ablation Sensor for Flight,” , 45th AIAA Aerospace Sciences Meeting and Exhibit, 9-12 January 2008, Reno, NV.

[6] K. Trumble, I. Cozmuta, S. Sepka, P. Jenniskens, M. Winter Post-flight Aerothermal Analysis of the Stardust Sample Return Capsule, Journal of Spacecraft and Rockets, Vol. 47, No. 5, pp. 765-764, September-October 2010.

[7] D. Empey, K. Skokova, P. Agrawal, G. Swanson, D. Prabhu, K. Peterson, M. Winter, E. Venkatapathy, Small Probe Reentry Investigation for TPS Engineering (SPRITE), AIAA-2012-0215, 50th AIAA Aerospace Sciences Meeting, Nashville, Tennessee, 9 - 12 Jan 2012.

[8] Nawaz, Anuscheh, Philippidis, Daniel, and Ho, Thanh. “Setup and characterization of the 30 kW arc jet facility mARC,” 44th AIAA Thermophysics Conference, San Diego, CA., 2013.